Kyushu University Global COE Program
Journal of Novel Carbon Resource Sciences, Vol. 4, pp. 32-35, Sep. 2011

Synthesis of Magnesia as a Reusable Sorbent for Fluoride

Naoyuki Fukumoto[*1], Keiko Sasaki[*2], Sayo Moriyama[*1], Tsuyoshi Hirajima[*2]
[*1]Graduate School of Engineering, Kyushu University
[*2]Faculty of Engineering, Kyushu University

(Received June 29, 2011; accepted September 9, 2011)

Magnesium oxide was produced by calcination of $MgCO_3$ reagent at 1273 K for 1 h. The product was confirmed to be a single phase of MgO by XRD. After sorption of 9.98 mmol·L^{-1} fluoride ions, the solid residues were dried and calcined again at 1273 K for 1 h. Then the second sorption of fluoride was conducted in the same manner as in the first phase of sorption. All XRD peaks for products were assigned to MgO. The order of sorption density of fluoride (mol·L^{-1}) apparently seems to be dependent on the specific surface area. However, after normalization of the sorption density for the specific surface area (mmol·m^{-2}), Q' values were found to be different. In the CO_2-TPD curves for calcined products, a component, which has the maximum peak at 415 K, was considered to be responsible for removal of fluoride. The peak intensity was converted to basicity per specific surface area (as CO_2 μmol·m^{-2}). It was found there was a positive relation between the basicity and the removal efficiency of fluoride.

1. Introduction

Fluorine (F) is an essential element for animal mineralization of bones and formation of dental enamel. However, excess intake leads to physical disorders such as dental fluorosis, stiffened and brittle bones and joints, deformation in knee and hip bones and finally paralysis making the person unable to walk or stand[1]. The safe limit of fluoride in drinking waters is 1 mg·L^{-1}. In Japan, the environmental guideline of fluoride is 0.8 mg·L^{-1} for drinking waters and 8.0 mg·L^{-1} for industrial discharge[2]. Groundwater pollution is the result of intensively agriculture field, disposal of hazardous waters, mine drainages, semi-conductor and glass industry drainages and solid waters, sewage disposal, and surface impoundments among many other sources[3]. The authors have reported that magnesia (MgO), which is obtained by calcination of magnesite ($MgCO_3$) removes fluoride ions effectively by destructive sorption. The mineral resources of magnesia is limited and occur locally in China. Therefore, it is important to establish the technologies for chemical regeneration of these mineral resources. Several adsorbent materials have previously been tested in search of efficient and economical defluorinating agents, including activated alumina[4], activated carbon[5], lime[6], magnesium-aluminium oxide[7], serpentine[8], and layered double hydroxides (LDHs)[9]. Magnesium oxide is relatively a common material and can be obtained by calcination of magnesite, which is a natural mineral. Magnesium oxide has been investigated as a solid catalyst in the formation of alcohol. The conditions of calcination affect its reactivity. The purpose of this study was to examine the reactivity of MgO with fluoride in aqueous systems. In the present study, MgO-rich products from calcination at 1273 K were characterized, and the effect of chemical regeneration on the removal of fluoride in aqueous systems was investigated.

2. Experiments

Fig. 1 shows that the sequential scheme of sorption experiments. MgO-rich phases were produced by calcination of $MgCO_3$ (special grade, Sigma-Aldrich, St. Louis, MO, USA) for 1 h at 1273 K, and by calcination of the solid residues after sorption of fluoride, designated as MgO-I, MgO-II, MgO-III, MgO-IV and MgO-V. Solid residue for each step was also designated as Residue-I, Residue-II, Residue-III, Residue-IV and Residue-V respectively, as shown in Fig. 1. Calcined products were characterized by X-ray diffraction with CuKα, 40 kV, 20 mA (XRD, Multi Flex, Rigaku, Akishima, Japan), and scanning electron microscopy (SEM, VE-9800, KEYENCE, Osaka, Japan). The specific surface areas were determined by the seven-point N_2-adsorption BET method (AUTOSORB-1, YUASA, Osaka, Japan) and temperature programmed desorption curves (TPD, BELCAT-B, BEL JAPAN Inc., Toyonaka, Japan) using CO_2 as a probe gas. CO_2-TPD curves were measured with an increasing temperature gradient of 3.3 K·min^{-1} after degassing by heating the samples at 773 K. The data were analyzed with BELCAT Chem Master Ver. 2.3.9 (BEL JAPAN Inc., Toyonaka, Japan) to evaluate the basicity and the number of base sites of calcined products consisting mainly of MgO.

1.24~45.77 mmol·L^{-1} fluoride solutions at pH 6.09 were prepared using NaF (special grade, Wako, Osaka, Japan). For sorption experiments, 0.100 g calcined MgO-rich phase sorbents were added to 40 mL fluoride solutions, followed by shaking at 100 rpm and at 298 K. In preliminary experiments, it was confirmed that the equilibrium was achieved within 72 h under these conditions. After 72 h supernatants were filtered (0.45 μm) for determination of total concentrations of fluoride by an ion chromatography (DIONEX ICS-90, Osaka, Japan). Solid residues after sorption were also characterized by XRD and SEM in the same manner as for the sorbents before sorption.

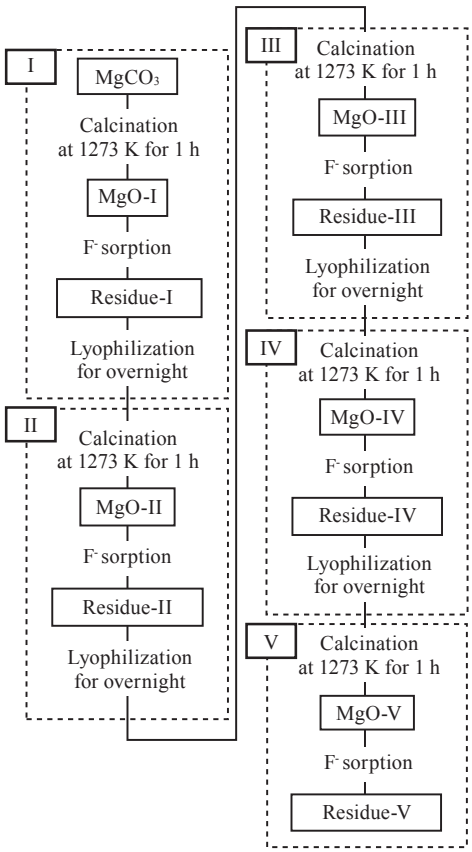

Fig. 1 Flow sheet of synthesis of MgO, sorption of fluoride, and calcination of solid residue.

3. Results and discussion

The specific surface areas (SSA) of the calcined products are listed in Table 1. The SSA was the largest for MgO-I. The second calcination resulted in a very low SSA, and after the third calcination the value increased gradually with the number of calcination cycles.

Table 1 SSA of the calcined products

Number of MgO	I	II	III	IV	V
SSA $m^2 \cdot g^{-1}$	29.1	1.5	2.3	5.1	7.1

Fig. 2 shows the XRD patterns of the MgO-I, MgO-V, Residue-I and Residue-V. In the calcined products, all peaks are assigned to MgO (JCPDS 45-946). For the solid residues, the major peaks are assigned to $Mg(OH)_2$ (JCPDS 44-1482) and MgO. Peak positions assigned to $Mg(OH)_2$ were identical to JCPDS 44-1482 in Residue-V, but shifted to left side in Residue-I. This might be caused by structural strain due to sorption of larger amounts of fluoride in Residue-I (Fig. 3). Peak intensities of $Mg(OH)_2$ were greater in Residue-I than Residue-V. The remaining peaks assigned to MgO can be also remarkably observed in Residue-V. The relative intensities of MgO in the solid residues increased with the number of regeneration cycles although the only MgO-I and MgO-V are shown here. These data indicate that the stability of MgO increased by calcination cycles.

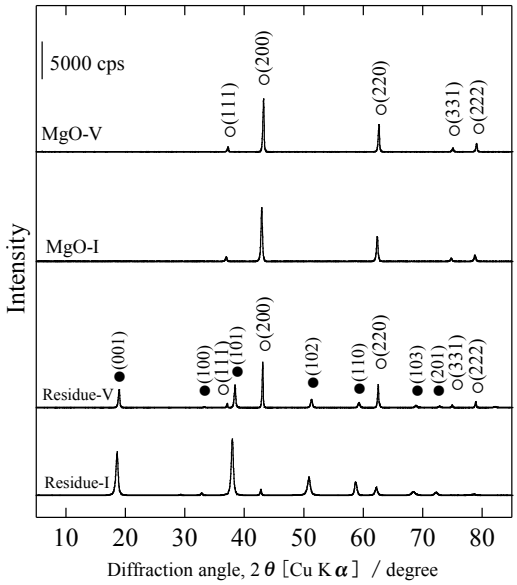

Fig. 2 XRD patterns of MgO-I, MgO-V, Residue-I and Residue-V after sorption of 9.82 $mmol \cdot L^{-1}$ fluoride. Symbols: ○, MgO (JCPDS 45-946); ●, $Mg(OH)_2$ (JCPDS 44-1482).

Fig. 3 shows the sorption isotherm of fluoride on the calcined products at 298 K. The amount of sorption of fluoride on the calcined product (Q in $mmol \cdot g^{-1}$) was maximum with MgO-I, minimum with MgO-II, and then increased with the calcination cycles. The capacity, Q was a function of the SSA. Therefore, by converting the Q value to Q' ($mmol \cdot m^{-2}$), a different trend could be seen as shown in Fig. 4. Because of the relationship with SSA, the Q' value was at maximum with MgO-II and at minimum with MgO-I. This estimation suggests that the sorbent, which has strong basicity, showed high affinity for fluoride. To clarify these findings, the bacisity and the number of base sites per SSA were measured.

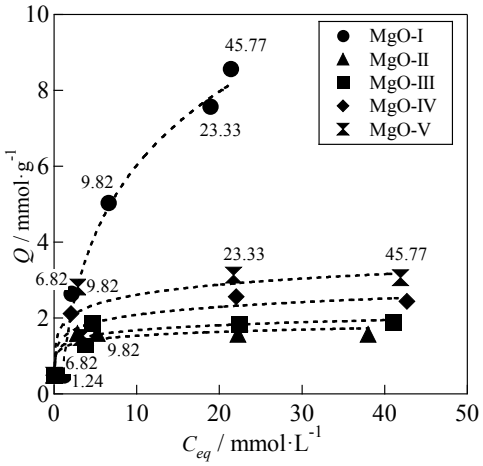

Fig. 3 Sorption isotherms of fluoride at 298 K on calcined produced by repeated calcination. The numbers indicate the initial F^- concentrations in $mmol \cdot L^{-1}$.

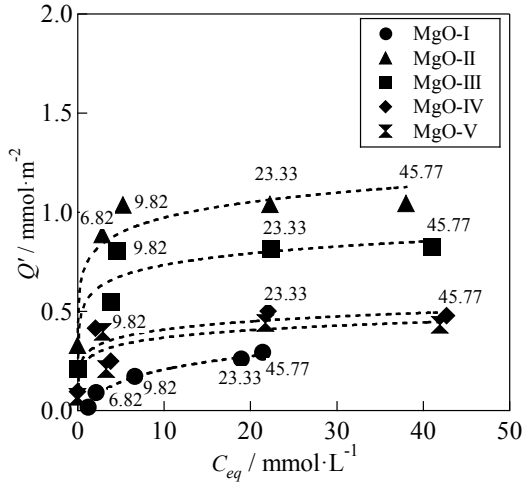

Fig. 4 Sorption isotherms of fluoride at 298 K on calcined produced per SSA. The numbers are the same as in Fig. 3.

The CO_2-TPD curves were collected in a range of 300 K to 700 K of CO_2-desorption temperature (Fig. 5). The peak positions of CO_2-TPD for MgO are in good agreement with the previous report[10]. The curves in Fig. 5 can be separated into three components with different basicities in the calcined products including mainly MgO. Although the TPD curves in Fig. 5 were obtained using electroconductivity as a detector, the analogical samples were separately determined using a quantity mass spectrometer (Q-mass). According to the results using Q-mass, it was confirmed that the first component (a) at 415 K is from CO_2 and the second and third components are from H_2O. Sorbed CO_2 quantities at the component of (a) in Fig. 5 are summarized in Table 2. There is an association between the basicity per SSA of the calcined products and the removal efficiency of fluoride as depicted in Fig. 6, although some fluctuation can be observed. The fluctuation might be derived from representativeness of samples, because only 0.100 g is provided for both CO_2-TPD and sorption experiments.

It is clear that the total surface area of calcined products, mainly MgO, is not so important for precipitation of $Mg(OH)_2$, because the initial surface area is immediately changed by coverage with precipitates. The larger basicity might lead the higher reactivity with H_2O as shown in the following equation[11), 12), 13)].

$$\equiv MgO + H_2O \rightleftarrows \equiv Mg^{\delta+}\!<\!\begin{matrix}O\!<\!\begin{matrix}H\\H\end{matrix}\\O_{\delta-}\end{matrix} \rightleftarrows \equiv Mg\!<\!\begin{matrix}OH\\OH\end{matrix} \qquad (1)$$

Fig. 7 shows SEM images for MgO-I, MgO-V, Reside-I and Residue-V. The MgO-I particles (Fig. 7(a)) of fluoride were rod shaped 10~20 μm in length and 5~6 μm in diameter. The surface of Residue-I (Fig. 7(b)) was totally covered with very fine flakes leading to increase in diameters, probably $Mg(OH)_2$ precipitates. The surface of MgO-V (Fig. 7 (c)) was covered with a lot of granular mass of 0.5~1.0 μm in length. MgO-II, MgO-III and

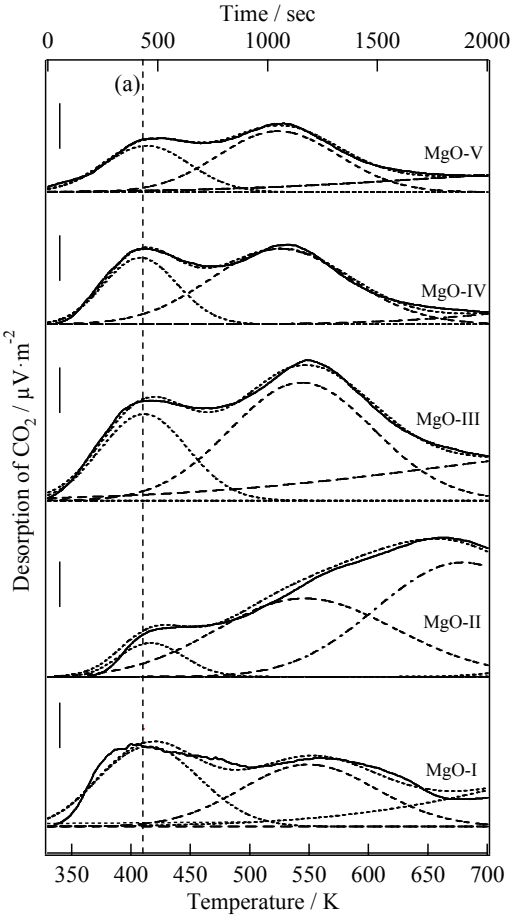

Fig. 5 CO_2-TPD curves of calcined products at different calcination cycles. Scale bars indicate 10 μV·m^{-2} for MgO-I, 250 μV·m^{-2} for MgO-II, 100 μV·m^{-2} for MgO-III, 50 μV·m^{-2} for MgO-IV and MgO-V.

Table 2 CO_2 sorption on the component (a) in Fig. 5

Number of MgO	I	II	III	IV	V
CO_2 μmol·m^{-2}	1.82	16.67	19.57	6.47	5.07

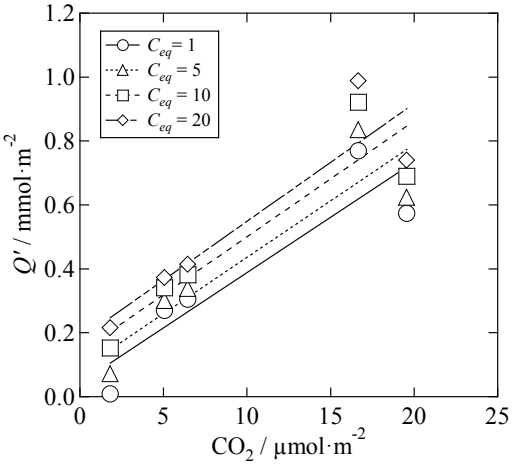

Fig. 6 Plots of *Q'* against sorbed CO_2. The numbers indicate C_{eq} (mmol·L^{-1}) calculated using the fitting in Fig. 4.

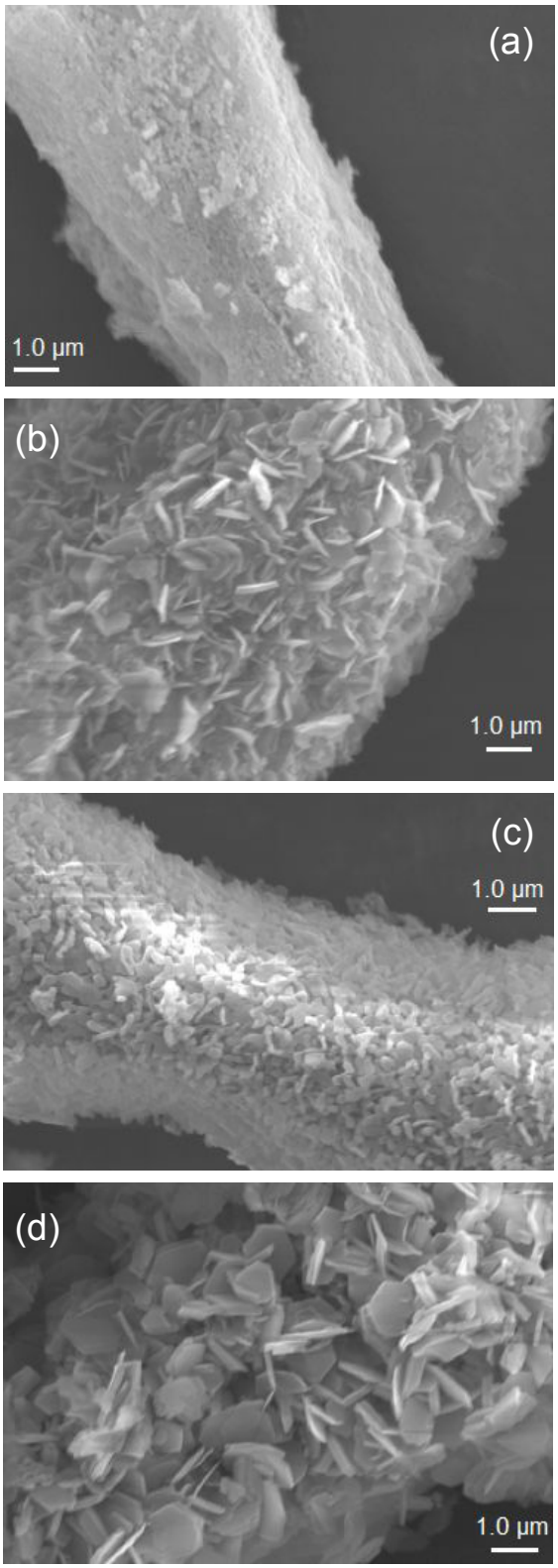

Fig. 7 SEM images of MgO-rich phases before and after sorption of 9.82 mmol·L^{-1} fluoride. (a) MgO-I, (b) Residue-I, (c) MgO-V, (d) Residue-V. Scale bars indicate 1.0 μm. Accelerating voltage is 15 kV.

MgO-IV had similar morphologies to MgO-V (data not shown). In SEM images of Residue-V (Fig. 7(d)), well-developed hexagonal flakes were observed on the surface consisting of $Mg(OH)_2$. As shown in Fig. 2, a phase of MgO still remained in Residue-V and peak shifts of $Mg(OH)_2$ were remarkably observed in Residue-I. Larger amounts of fluoride were sorbed on MgO-I than MgO-V as shown in Fig. 3. Comprehensively considering these facts, it is suggested that $Mg(OH)_2$ crystals including much more fluoride look less developed flakes in SEM images (Fig. 7) and lead increase in lattice parameters for Residue-I (Fig. 2), while Residue-V includes less impurities of fluoride ions leading well developed crystals of $Mg(OH)_2$, which are reflected to XRD and SEM. The repetition of calcination makes well crystalline MgO in cores of grains, resulting in remaining phase of MgO even after sorption in the same conditions.

4. Conclusion

Reactivity of fluoride with MgO was investigated using sorption isotherm at 298 K in five times of repeat of calcination and sorption under the same conditions. Repeating times of calcinations did not show a clear trend of neither SSA of calcined products nor sorption efficiency of fluoride per unit mass and surface area. Sorption efficiency was not clearly related with SSA.

However, the positive correlation was found between sorbed mass of fluoride per SSA (*Q'*) and sorption capacity of CO_2 as an indicator of basicity which was obtained from CO_2-TPD analysis. The basicity on the surface of MgO affects to reactivity with H_2O resulting in removal efficiency of fluoride during co-precipitation of fluoride with $Mg(OH)_2$. Increase in calcinations times lead well crystalline MgO in cores of grains but it did not always increase the total basicity of the surface of MgO particle.

This result gives a prospect that sequential system and calcinations condition in each step should be optimized to maximize the total efficiency of sorption of fluoride in practical cases.

References

1) O. Oren, Y. Yechieli, J. K. Bohlke, A. Dody, *J. Hydrol*, **49**(6), 312 (2004).
2) M. C. Bell, T. G. Ludwig, *WHO Monogr. Ser. 59*, (1970).
3) F. Anwar, *Waste Manag*, **23**(9), 817 (2003).
4) P. L. Bishop, G. Sansoucy, *J. AWWA*, **70**, 554 (1978).
5) K. Muthukumaran, N. Balasubramanian, *J. Environ.*, **15**(7), 514 (1995).
6) W. Rongshu, H. Li, P. Na, W. Ying, *Water Qual. Res. J. Can.*, **30**(1), 81 (1995).
7) T. Kameda, N. Uchiyama, K. S. Park, G. Grause, T. Yoshioka, *Chemosphere*, **73**, 844 (2008).
8) C. D. Nava, M. S. Rois, M. T. Olguin, *Separ. Sci. Technol.*, **38**(1), 131 (2003).
9) L. Lv, J. Hea, M. Wei, D. G. Evans, X. Duan, *J. Hazard. Mater.*, **B133**, 119 (2006).
10) S. Fan, N. Zhao, J. Li, F. Xiao, W. Wei, Y. Sun, *Catal. Lett.*, **120**, 299 (2008).
11) M. E. Martin, R. M. Narske, K. J. Klabunde, *Micro. Meso. Mater.*, **83**, 47 (2005).
12) M. Okazaki, S. D. Kimura, T. Kikuchi, M. Igura, T. Hattori, T. Abe, *J. Hazard. Mater.*, **154**, 287 (2008).
13) K. Sasaki, N. Fukumoto, S. Moriyama, T. Hirajima, *J. Hazard. Mater.*, **191**, 240 (2011).